

HeadArtist: Text-conditioned 3D Head Generation with Self Score Distillation

Hongyu Liu*
hliudq@cse.ust.hk
HKUST
Hong Kong, China

Xuang Wang[†]
Ant Group
Hang Zhou, China

Ziyu Wan
City University of Hong Kong
Hong Kong, China

Yujun Shen
Ant Group
Hang Zhou, China

Yibing Song
Alibaba DAMO Academy
Hang Zhou, China

Jing Liao
City University of Hong Kong
Hong Kong, China

Qifeng Chen[†]
HKUST
Hong Kong, China
cqf@ust.hk



Figure 1: Generation and editing results of our HeadArtist with text guidance, regarding both realistic and virtual characters. † and ‡ denote the prefixes “a head of ...” and “a DSLR portrait of ...”, respectively. Text in orange denotes the editing instruction.

*This work is done partially when Hongyu is an intern at Ant Group.

[†]Joint corresponding authors.

Permission to make digital or hard copies of all or part of this work for personal or classroom use is granted without fee provided that copies are not made or distributed for profit or commercial advantage and that copies bear this notice and the full citation on the first page. Copyrights for components of this work owned by others than the author(s) must be honored. Abstracting with credit is permitted. To copy otherwise, or republish, to post on servers or to redistribute to lists, requires prior specific permission and/or a fee. Request permissions from permissions@acm.org.

SIGGRAPH Conference Papers '24, July 27-August 1, 2024, Denver, CO, USA

© 2024 Copyright held by the owner/author(s). Publication rights licensed to ACM.

ACM ISBN 979-8-4007-0525-0/24/07...\$15.00

<https://doi.org/10.1145/3641519.3657512>

ABSTRACT

We present HeadArtist for 3D head generation following human-language descriptions. With a landmark-guided ControlNet serving as a generative prior, we come up with an efficient pipeline that optimizes a parameterized 3D head model under the supervision of the prior distillation itself. We call such a process **self score distillation (SSD)**. In detail, given a sampled camera pose, we first render an image and its corresponding landmarks from the head model, and add some particular level of noise onto the image. The noisy image, landmarks, and text condition are then fed into a frozen ControlNet

twice for noise prediction. We conduct two predictions via the same ControlNet structure but with different classifier-free guidance (CFG) weights. The difference between these two predicted results directs how the rendered image can better match the text of interest. Experimental results show that our approach produces high-quality 3D head sculptures with rich geometry and photo-realistic appearance, which significantly outperforms state-of-the-art methods. We also show that our pipeline supports editing operations on the generated heads, including both geometry deformation and appearance change. Project page: <https://kumapowerliu.github.io/HeadArtist>.

CCS CONCEPTS

• **Computing methodologies** → **Rendering; Learning paradigms; Mesh models.**

KEYWORDS

3D Head Generation, 3D Head editing, Text Guided, Self Score Distillation

ACM Reference Format:

Hongyu Liu, Xuang Wang, Ziyu Wan, Yujun Shen, Yibing Song, Jing Liao, and Qifeng Chen. 2024. HeadArtist: Text-conditioned 3D Head Generation with Self Score Distillation. In *Special Interest Group on Computer Graphics and Interactive Techniques Conference Conference Papers '24 (SIGGRAPH Conference Papers '24)*, July 27-August 1, 2024, Denver, CO, USA. ACM, New York, NY, USA, 17 pages. <https://doi.org/10.1145/3641519.3657512>

1 INTRODUCTION

Advancements in vision-language models have significantly propelled the development of AIGC via human language descriptions, including text-to-image [Nichol et al. 2021; Ramesh et al. 2022, 2021; Rombach et al. 2022; Saharia et al. 2022; Yu et al. 2022], text-to-video [Esser et al. 2022; Ho et al. 2022; Singer et al. 2022; Wu et al. 2023a], and text-to-3D generation [Lin et al. 2023; Mendiratta et al. 2023; Metzger et al. 2023; Poole et al. 2022; Wang et al. 2023a,b]. Among these applications, text-to-3D head generation receives tremendous attentions. As part of the text-to-3D generation, modeling 3D head avatars holds significant potential in various areas including augmented reality, virtual reality, game character creation, and real-time interaction.

There are several investigations [Wang et al. 2023c; Yu et al. 2023; Zhang et al. 2023a] to generate text-guided human heads. Usually, they train a 3D generative model (i.e., Diffusion model [Ho et al. 2020] or GAN [Goodfellow et al. 2014]) by using datasets consisting of text-image pairs. With implicit 3D representations residing in these datasets, human heads are effectively generated. However, the performance of these methods hinges on high-precision dataset acquisition, and the generated heads sometimes lack diversity.

On the other hand, certain methods [Cao et al. 2023; Chen et al. 2023; Han et al. 2023; Huang et al. 2023b; Zhang et al. 2023b] employ pre-trained text-to-image diffusion models to generate 3D heads, thereby are not limited by the dataset constraint and their results are more diverse. Specifically, they utilize Score Distillation Sampling [Poole et al. 2022] (SDS) to optimize 3D head parameters with a pre-trained diffusion model. Facial landmarks [Lugaresi et al. 2019] or 3D Morphable Models [Blanz and Vetter 2003; Li et al. 2017] (3DMM) are incorporated to enhance the generated

outputs. However, these approaches cannot avoid limitations inherent to SDS, such as over-saturation and over-smoothing. Recently, Variational Score Distillation [Wang et al. 2023b] (VSD) treats 3D parameters as random variables instead of constant data points as that in SDS. In this way, VSD can effectively address texture issues from SDS by utilizing normal CFG weights [Ho and Salimans 2022] (i.e., $\omega = 7.5$). However, VSD may not produce satisfactory results when optimizing geometry for 3D head generation. This is because VSD does not introduce a geometric structure prior of human heads (e.g., facial component). Moreover, both SDS and VSD may produce multi-face Janus artifacts on the 3D human heads. These artifacts reduce the fidelity and authenticity of the generated results.

In this paper, we present HeadArtist to distill 3D heads within a 3D head-aware diffusion model, by leveraging a frozen landmark-guided ControlNet [Zhang et al. 2023e]. Specifically, our method disentangles the generation process into geometry and texture generations. Besides, we utilize the DM Tet mesh [Shen et al. 2021] initialized with the Flame model [Li et al. 2017] as our 3D head representation. Given a camera pose, we render an image and project the corresponding landmarks from the 3D head on it. We add noise to this rendered image, and combine this image with landmarks and text prompts to constitute our model inputs. These inputs are then fed into the ControlNet twice, enabling us to predict two types of noises. The first type of noise which is predicted by setting CFG as 1, represents the distribution score of the generated 3D head. We set another type of noise that is predicted by setting CFG as 7.5 and 100 for texture and geometry, respectively. This type of noise represents the distribution score of the target 3D head. Our objective is to minimize the score difference between these two distributions for 3D head parameter optimizations. We name this process “self-score distillation”. It represents the self-supervision of ControlNet on our 3D generation model. Intuitively, our SSD has two advantages: (1) As both of these two noises are sampled from the same ControlNet and landmarks, there is a direct spatial alignment of these two scores. This alignment effectively suppresses the occurrence of multi-face Janus artifacts to help us generate high-quality geometry; (2) As the landmarks already contain good facial structure priors, we use the ControlNet to naturally incorporate a 3D head prior during our generation process.

After generating a 3D head, we can manipulate both its geometry and texture by following human language descriptions. During manipulation and generation, direct use of negative text prompts can greatly enhance texture realism and intricacy. In Figure 1, we show that our head results are of premier quality from the perspective of geometry and texture.

2 RELATED WORKS

In this section, we first discuss the progress of Text-to-3D generation on general objects. Then, we focus on the Avatar generation including human heads and human bodies.

2.1 Text-to-3D General Object Generation

There has been a remarkable advancement in text-to-2D image generation [Nichol et al. 2021; Ramesh et al. 2022, 2021; Rombach et al. 2022; Saharia et al. 2022; Yu et al. 2022; Zhu et al. 2022]. These methods advance the text-to-3D content generation [Lin

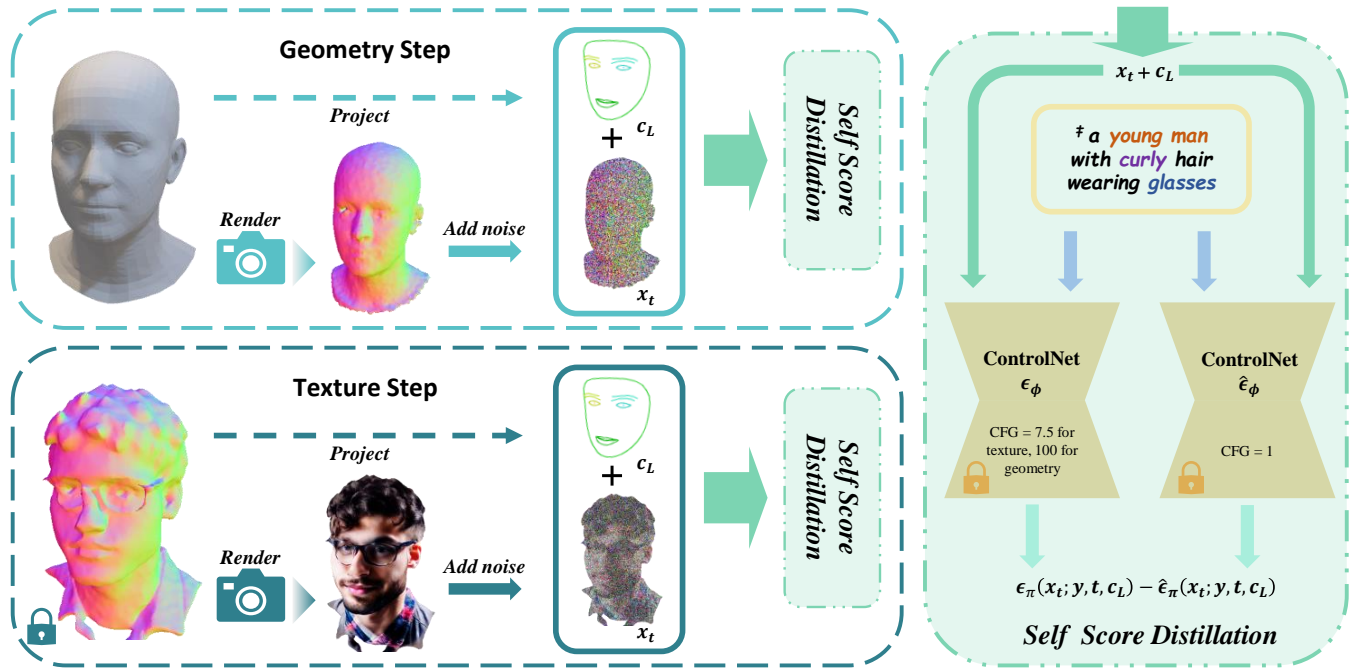


Figure 2: We conduct two steps to generate geometry and textures, respectively. For the geometry step, we employ DMTet mesh [Shen et al. 2021] initialized by Flame [Li et al. 2017] as a representation of 3D human head’s geometry. For the texture step, we fix the generated geometry and construct a texture space based on DMTet. The texture space construction is similar to that in Magic3D [Lin et al. 2023]. In these two steps, we project mesh keypoints to get landmarks guided by a camera. Afterward, we render a normal map and a texture in these two steps for model training via our self-score distillation, the x_t in these two steps are the normal map and texture with noise respectively.

et al. 2023; Poole et al. 2022; Sanghi et al. 2022; Wang et al. 2022, 2023b]. Currently, text-to-3D methods generally use pre-trained text-to-2D image models to guide the generation process. One type of approaches [Jain et al. 2022; Michel et al. 2022; Sanghi et al. 2022; Wang et al. 2022] adopt the CLIP [Radford et al. 2021] loss as supervision for model training. Due to the lack of spatial representation in CLIP, these methods contain challenges to producing authentic content. On the other hand, there is another type of approaches [Liang et al. 2023; Lin et al. 2023; Liu et al. 2023a; Metzger et al. 2023; Qian et al. 2023; Qiu et al. 2023; Sun et al. 2023; Tang et al. 2023] that leverage pre-trained diffusion models as supervision and utilize loss functions such as SDS [Poole et al. 2022; Wang et al. 2023a] to distill 3D parameters [Mildenhall et al. 2021; Shen et al. 2021; Wang et al. 2021]. While these approaches have achieved promising results, they suffer from the inherent problems of SDS, such as over-saturation, over-smoothing, and multi-face Janus artifacts. More recently, VSD [Wang et al. 2023b] proposes a principled particle-based variational framework to generate realistic textures with normal classifier-free guidance weights. However, the VSD needs SDS to optimize the geometry, and it also contains multi-face Janus artifacts.

2.2 Text-to-3D Avatar Generation

Apart from text-to-3D general object generation, several methods focus on text-to-3D Avatar Generation. Studies [Wang et al. 2023c;

Zhang et al. 2023a] adopt the diffusion model [Ho et al. 2020] and generative adversarial networks [Goodfellow et al. 2014] to produce the 3D head avatar. DreamFace [Zhang et al. 2023d] utilizes a component selection within the CLIP to generate preliminary geometry and employs SDS with a diffusion model to refine UV texture. Despite the impressive performance, these methods heavily rely on well-annotated datasets. These datasets are challenging to acquire and constrain the generation diversity.

Differently, several methods leverage pre-trained text-to-image models for supervising the training process without data dependence. Specifically, some methods [Aneja et al. 2023; Hong et al. 2022] use the CLIP loss [Radford et al. 2021] to supervise the training process. They adopt the SMPL-X [Pavlakos et al. 2019] and Flame [Li et al. 2017] as the geometry prior, respectively. These methods effectively generate corresponding avatars according to different texts and in different styles. DreamAvatar [Cao et al. 2023], DreamHuman [Kolotouros et al. 2023] and Avatarfusion [Huang et al. 2023b] distillate a 3D avatar from a pre-trained 2D text-to-image diffusion model with SDS loss. They also apply some existing geometry parametric models to initialize the avatar shape. Moreover, a 3D aware diffusion model is trained in [Huang et al. 2023a; Zeng et al. 2023; Zhang et al. 2023b] to replace the pre-trained 2D diffusion model for achieving better performance. Meanwhile, some methods [Huang et al. 2023c; Liu et al. 2023b; Shi et al. 2023; Wu et al. 2023b; Yuan et al. 2023; Zhang et al. 2023c] use an image

accompanied with the text as guidance to increase model robustness. More recently, Head Sculpt [Han et al. 2023] introduces the prior-driven score distillation with landmark-guided ControlNet to improve 3D-head generations. Although these methods leverage SDS to generate realistic avatars, they cannot avoid intrinsic limitations associated with SDS. In this paper, we propose self-score distillation (SSD) to generate both geometry and texture for a substantial performance improvement.

3 PRELIMINARY

In this section, we provide a brief overview of some essential prerequisites that are closely related to our HeadArtist in Section 4. We denote ϵ_ϕ as a pretrained text-to-2D diffusion model, θ as the parameters of a 3D representation (i.e., NeRF), R as a differentiable rendering function and y as the text prompt.

3.1 Score Distillation Sampling

DreamFusion [Poole et al. 2022] first proposes Score Distillation Sampling (SDS) that utilizes a pretrained text-to-2D diffusion model ϵ_ϕ to distill θ . Specifically, for a rendered image $x = R(\theta, c)$ from a 3D model with a camera c , they first add a Gaussian noise $\epsilon \sim \mathcal{N}(0, 1)$ to this image to get x_t at time t during the forward diffusion process. Then, they simulate the training process of the diffusion model to minimize the distance between the added noise ϵ and the predicted noise by using the pre-trained diffusion model. The gradient of SDS is computed as:

$$\nabla_\theta \mathcal{L}_{\text{SDS}}(R(\theta)) = \mathbb{E}_{t, \epsilon} \left[\omega(t) (\epsilon_\phi(x_t; y, t) - \epsilon) \frac{\partial x}{\partial \theta} \right], \quad (1)$$

where $\omega(t)$ is a time-dependent weighting function. In practice, SDS utilizes the classifier-free guidance [Ho and Salimans 2022] (CFG) to adjust the sampling direction, which slightly deviates from unconditional sampling, i.e., $\epsilon_\phi(x_t; y, t) + W(\epsilon_\phi(x_t; y, t) - \epsilon_\phi(x_t; t, \emptyset))$, where \emptyset represents the ‘‘empty’’ text prompt, and W is the CFG weight. The results show that SDS significantly improves text-to-3D performance. However, SDS is prone to produce over-saturated and over-smoothed results as shown in DreamFusion [Poole et al. 2022]. This is because SDS needs a large CFG weight (i.e., $W = 100$) for stable training. Also, SDS results contain multi-face Janus artifacts.

3.2 Variational Score Distillation

Recently, ProlificDreamer [Wang et al. 2023b] considers θ as a random variable rather than a single point in SDS and proposes Variational Score Distillation (VSD). The VSD can use the normal CFG guidance weight (i.e., $W = 7.5$) to get the distribution of high-quality results during training. Specifically, given a target text prompt y , there is a rendering image distribution $q^\mu(x|y)$ of 3D representations $\mu(\theta|y)$ conditioned by this prompt. VSD tries to align this distribution with a real image distribution of $t = 0$ defined by the pretrained text-to-image diffusion model under KL divergence as follows:

$$\mathcal{L}_{\text{VSD}} = \min_{\mu} D_{\text{KL}}(q^\mu(x|y, c) \| p(x|y)). \quad (2)$$

To solve Eq. 2, VSD formulates this optimization as the combination of different diffusion distributions indexed by t . Then, VSD calculates the distance between the distribution score of real and

rendered images at time t as below:

$$\nabla_\theta \mathcal{L}_{\text{VSD}}(R(\theta)) = \mathbb{E}_{t, \epsilon} [\omega(t) (\epsilon_\phi(x_t; y, t) - \epsilon_{\text{loRa}}(x_t; y, t, c)) \frac{\partial x}{\partial \theta}], \quad (3)$$

where ϵ_{loRa} , a LoRA (Low-rank adaptation) [Hu et al. 2021] model based on ϵ_ϕ , represents the distribution of the rendered image. The LoRA model is trained by using the rendered image x , text prompt y , and camera pose c to minimize the difference $\|\epsilon_{\text{loRa}}(x_t, y, t, c) - \epsilon\|_2^2$. However, optimizing the geometry of θ directly with VSD is challenging and requires the guidance of SDS. Moreover, the training process of LoRA is unstable and ineffective in obtaining an accurate representation of the current 3D distribution. So more time is taken for model training to converge. In addition, generating the 3D head directly using VSD is difficult due to the absence of a 3D head structure prior. With these observations, our method tries to address these issues with self score distillation.

3.3 3D Representation

We follow Fantasia3D [Chen et al. 2023] to disentangle the geometry and texture. For the geometry, we use DM Tet [Shen et al. 2021] as our geometry representation. Specifically, DM Tet maintains a deformable tetrahedral grid (V_T, T) where V_T are vertices. For each vertex $v_i \in V_T$, DM Tet predicts a Signed Distance Function (SDF) value and a position offset from a learned MLP module. Subsequently, the SDF can be transferred to a mesh with a differentiable Marching Tetrahedral layer. With the DM Tet mesh, we can efficiently render high-resolution textures for fast training with effective detail preservation.

4 PROPOSED METHOD

Head-Artist generates high-fidelity 3D heads following language descriptions. Figure 2 shows an overview where our framework is divided into two steps: geometry and texture optimization steps. In the texture optimization step, we fix the optimized mesh as the shape guidance. The whole optimization process is conducted by self score distillation. Overall, our HeadArtist generates diverse 3D heads ranging from real individuals to virtual characters. The generated 3D heads contain intricate geometry and high-fidelity textures. The detailed illustration is shown below:

4.1 Self Score Distillation

The general objects are generated well by SDS and VSD. For 3D human heads, these two methods encounter substantial challenges as shown in Figure 3. This is because 3D heads contain two unique characteristics apart from general objects: 1) Unlike general objects such as hamburgers with viewpoint-invariant properties, 3D heads exhibit obvious view discrepancy across different poses. The view discrepancy makes the generation more susceptible to multi-face Janus artifacts; 2) The facial region of 3D heads contains highly structured semantic components (i.e., eyes, nose, and mouth). These components have been precisely identified. Therefore, the pose and facial components are important guidance and contribute to the 3D head generation process. Although HeadSculpt [Han et al. 2023] leverages a 3D-head-aware diffusion model, it introduces SDS to

generate 3D heads. As such, the inherent limitations of SDS (i.e., over-saturation and over-smoothing) will affect its output result.

We propose Self Score Distillation (SSD) to obtain a 3D head distribution within a pre-trained 3D head-aware diffusion model. Specifically, there is a distribution of a rendered image $q^{\mu_h}(\mathbf{x}|y, c)$ with optimized 3D head distribution $\mu_h(\theta|y)$. Also, we can obtain a pre-trained 3D-head-aware diffusion model to get a real image distribution $p(\mathbf{x}|y, c)$ with a text and camera pose. Finally, our self score distillation aims to minimize the following KL divergence:

$$\mathcal{L}_{\text{SSD}} = \min_{\mu_h} D_{\text{KL}}(q^{\mu_h}(\mathbf{x} | y, c) \| p(\mathbf{x} | y, c)). \quad (4)$$

Inspired by VSD and SDS, to address the above KL divergence, we can set up a series of optimization objectives characterized by varying marginal diffused distributions indexed by t :

$$\mathcal{L}_{\text{SSD}} = \min_{\mu_h} D_{\text{KL}}(q_t^{\mu_h}(\mathbf{x}_t | y, t, c) \| p_t(\mathbf{x}_t | y, t, c)). \quad (5)$$

To solve Eq. 5, we need two 3D-head-aware diffusion models to represent the distribution of $q_t^{\mu_h}$ and p_t , respectively, so that we can sample x_t based on camera and text. For p_t , we employ a pre-trained landmark-guided ControlNet. This ControlNet is trained on a comprehensive 2D facial dataset [CrucibleAI 2023; Zheng et al. 2022], where the ground-truth data is generated by rendering facial landmarks from MediaPipe [Lugaresi et al. 2019]. The incorporation of ControlNet allows us to obtain x_t with multi-view consistency since we can denote the landmark as a camera pose. To compute $q_t^{\mu_h}$, one possible approach is to train a LoRA model to make a prediction like what VSD does. However, the training process of LoRA is unstable. Even though we assume LoRA has been trained well, the mismatch between LoRA and ControlNet makes the learned LoRA hard to align these two distributions. The mismatch is caused by these two diffusion models that adopt the conventional camera parameters and landmarks as head pose, respectively. Moreover, it leads to the emergence of the multi-face Janus artifact, as depicted in column (c) of Figure 5.

Fortunately, we observe that the ControlNet itself is trained on a meticulously aligned dataset consisting of facial landmarks, text, and face images. The accurate alignment enables ControlNet to naturally represent $q_t^{\mu_h}$ and sample x_t . The x_t is the marginal distribution of the ControlNet given the text and landmarks. Different from LoRA, the ControlNet incorporates landmarks that provide significantly richer semantic information for human facial regions than only using camera parameters. The gradient of \mathcal{L}_{SSD} can be written as

$$\nabla_{\theta} \mathcal{L}_{\text{SSD}}(R(\theta)) = \mathbb{E}_{t, \epsilon} [\omega(t)(\epsilon_{\pi}(\mathbf{x}_t; y, t, c_L) - \hat{\epsilon}_{\pi}(\mathbf{x}_t; y, t, c_L)) \frac{\partial \mathbf{x}}{\partial \theta}], \quad (6)$$

where c_L is the landmark, ϵ_{π} and $\hat{\epsilon}_{\pi}$ represent two pre-trained and frozen Controlnets with the same parameters. In practice, we employ CFG = 1 for $\hat{\epsilon}_{\pi}$ to estimate the score of the optimized 3D head distribution based on the text. Meanwhile, we set different CFG weights for predicting the score of the real image distribution of geometry and texture. The detailed settings are illustrated in the next subsection. In general, we iteratively conduct the training process by using ControlNet with self-distillation. Two predicted noises are guided by the same landmarks, which ensures an accurate alignment.

In comparison to SDS and VSD, Our SSD offers two advantages: 1) we obtain two distribution scores from the same diffusion model via identical landmarks as shown in Eq. 6, which ensures accurate spatial alignment to address the multi-face Janus issue; 2) we introduce landmarks for 3D head generation. The landmarks benefit 3D heads as they naturally bring facial semantic features. By leveraging these two advantages, our method exhibits superior performance for 3D head generation.

4.2 Head Generation

We generate high-fidelity 3D heads via SSD training. Specifically, we first generate the geometry, then we fix the geometry as guidance to generate the texture.

4.2.1 Geometry Generation. We follow Fantasia3D to adopt the DM Tet as our geometry representation and initialize it with the Flame model. Specifically, the DM Tet is parametrized via an MLP module ψ_g . For each vertex v_i in a deformable tetrahedral grid (V_T, T) , we use the MLP to predict SDF s_{v_i} and offset Δv_i . We randomly sample a point set $\{p_i \in \mathbb{R}^3\}$ and get SDF value $\text{Flame}_{\text{SDF}}(p_i)$ in the Flame model, then we use the following loss to optimize ψ_g : $\sum_{p_i \in P} \|s(p_i) - \text{Flame}_{\text{SDF}}(p_i)\|_2^2$.

After initialization, given a camera, we use the differentiable render (e.g., nvidiffrast [Laine et al. 2020]) to generate the normal map n , and we project the specific vertices of Flame into a landmark map c_L . Then we add Gaussian noise to n to get x_t and use our SSD to optimize ψ_g of DM Tet. Moreover, since there is a domain gap between the normal map and the real image which is used to train ControlNet, we set the $W = 100$ (CFG) for ControlNet ϵ_{π} to stabilize training. Meanwhile, we render the opacity mask combined with the normal map in the early stages of optimization.

4.2.2 Texture Generation. During the texture generation process, the geometric structure remains fixed, while a neural color field is constructed via an MLP module. The MLP module is denoted as ψ_{tex} . The color field predicts the RGB value for each vertex in the geometry. Then, we render the color field to get the texture, and we add the noise to the texture to get the x_t . Meanwhile, we project the landmark with a fixed geometry structure. Finally, we send x_t , landmark, and text prompt to SSD to optimize the ψ_{tex} . For texture generation, we set $W = 7.5$ (CFG) for ϵ_{π} , which is the common setting for diffusion models to get high-fidelity results. Moreover, we have discovered that our SSD can effectively leverage the negative prompts (i.e., replacing the empty prompt in CFG with "worst quality, low quality, semi-realistic") for further performance improvement.

4.3 Head Editing

After high-quality 3D head generation, we can edit the generated head as a follow-up. The editing process contains two unique steps including geometric deformation and texture manipulation. Specifically, when users provide specific instructions to modify a generated head, we fix the SDF s_{v_i} and focus on learning the offset Δv_i for each vertex within DM Tet to achieve mesh deformation. Then, we fix the modified geometry, and continue to update parameters of ψ_{tex} which is already pretrained in the generation process. The

whole process is conducted by SSD with different text and landmarks. Since we establish a canonical space with fixed SDF values and the editing texture inherits from the previous generation, our final result can well preserve the identity of the original character.

5 EXPERIMENTS

In this section, we illustrate our implementation details. Then, we provide qualitative and quantitative evaluations. Finally, we perform an ablation study of our approach.

5.1 Implementation Details

Our Head-Artist employs the Stable-Diffusion based ControlNet [CrucibleAI 2023] within the Huggingface Diffusers [von Platen et al. 2022] with the version 2-1-base [stabilityai 2023]. The entire framework is constructed upon threestudio [Guo et al. 2023]. For both geometry and texture generation, we render normals and textures at a size of 512×512 . We conduct 15k and 20k iterations for geometry and texture training, respectively. Our training is performed on a single NVIDIA RTX A6000 GPU, with a batch size of 1. The total training time is around 3 hours with an AdamW optimizer. We follow the ProlificDreamer [Wang et al. 2023b] to utilize the annealed time schedule. During both texture and geometry generation, we follow the DreamFusion [Poole et al. 2022] and add the view-dependent text for the ControNet ϵ_π . Specifically, for the back-view, we exclude facial features in the landmark and solely project the head’s contour. We maintain a Hash Encoding [Müller et al. 2022] to embed the poison points during the whole generation process. We set the maximum time steps as 0.5 for the geometry generation, since the geometry is initialized with the Flame model and need not generate from the complete Gaussian noise. More implementation details and results can be found in the supplementary material.

We conducted comprehensive comparisons between our method and five approaches: DreamFusion [Poole et al. 2022], LatentNerf [Metzger et al. 2023], Fantasia3d [Chen et al. 2023], ProlificDreamer [Wang et al. 2023b], and HeadSculpt [Han et al. 2023]. For fair comparisons, we incorporated Flame as the geometry prior for both LatentNerf and Fantasia3d. All methods except HeadSculpt are implemented with threestudio. As the implementation of HeadSculpt is not available, we directly borrow their provided results.

5.2 Qualitative Evaluation

In Figure 3, we present the visual comparisons between our HeadArtist and other methods. When inspecting geometry, LatentNerf, DreamFusion, and ProlificDreamer suffer from the problem of multi-face Janus. The HeadSculpt and Fantasia3d try to overcome this problem by introducing the 3D head prior, but their geometry still contains artifacts (e.g., the hollowness around the eyes in C of Fantasia3D, and the geometry noise of the female in B of HeadSculpt). In contrast, our HeadArtist, with the spatial alignments guided by landmarks, resolves the issue of multiple head artifacts and achieves more accurate head geometry. When inspecting texture, due to the adoption of SDS during training, DreamFusion, LatentNerf, Fantasia3d, and HeadSculpt have either over-saturation or over-smooth issues. ProlificDreamer performs well in texture generation, but it has collapsed shapes with the multi-face Janus issue. In comparison,

Table 1: Quantitative comparisons of state-of-the-art methods. We conduct a user study to score the performance of the method, with a maximum score of 6 points. \uparrow indicates higher is better.

Method	CLIP-L/14 \uparrow	CLIP-B/32 \uparrow	User Study \uparrow
DreamFusion [Poole et al. 2022]	0.261	0.284	2.06
ProlificDreamer [Wang et al. 2023b]	0.264	0.316	2.45
LatentNerf [Metzger et al. 2023]	0.262	0.313	2.72
Fantasia3d [Chen et al. 2023]	0.271	0.312	3.47
HeadSculpt [Han et al. 2023]	0.280	0.323	4.56
Ours	0.300	0.334	5.67

Table 2: Quantitative evaluation of ablation study. The methods correspond one-to-one to the methods in Figure 5. \uparrow indicates higher is better.

Method	CLIP-L/14 \uparrow	CLIP-B/32 \uparrow
a	0.2590	0.2786
b	0.2132	0.2351
c	0.2655	0.2901
d	0.2797	0.2986
f	0.2893	0.3191
e	0.2998	0.3276

our HeadArtist with SSD demonstrates more photorealistic texture generations. To sum up, our method generates human head geometries that are both plausible and free of artifacts, and the texture is remarkably realistic. Moreover, the generated results closely align with human-language descriptions.

In addition to generation, our method is effective in editing. As depicted in Figure 1 and Figure 4, with text instructions, we can effectively make corresponding manipulations to the geometry and texture simultaneously. Our method enables the manipulation of various head attributes (i.e., expressions, age, and style), while effectively preserving the character identity.

5.3 Quantitative Evaluation

We conduct a user study to evaluate the robustness of our method using 10 text prompts, which are from HeadSculpt. Based on these text prompts, we compare the generated heads which are rendered into freely viewable videos showing both geometry and textures. We invite 10 participants with computer graphics backgrounds to rate each result with a score from 1 to 6 (the higher the score, the better the effect). We calculate the average score for each method. Table 1 shows the subjective evaluation performance where our method is more favorable.

In addition to the user study, we further evaluate the relevance of text prompts and 3D heads by using the CLIP score [Radford et al. 2021]. We use two CLIP models, including CLIP-B/32 and CLIP-L/14, to do the evaluation. We convert videos used in the User Study into images, and then feed these images, along with their corresponding texts, into the CLIP model to compute the scores. The results, as shown in Table 1, indicate that our method is capable of generating 3D head models that exhibit a better alignment with the text prompts.

5.4 Ablation Study

5.4.1 Effectiveness of SSD. We conduct different configurations in Figure 5 to evaluate our SSD. In (a), we replace ϵ_π and $\hat{\epsilon}_\pi$ with a 2D

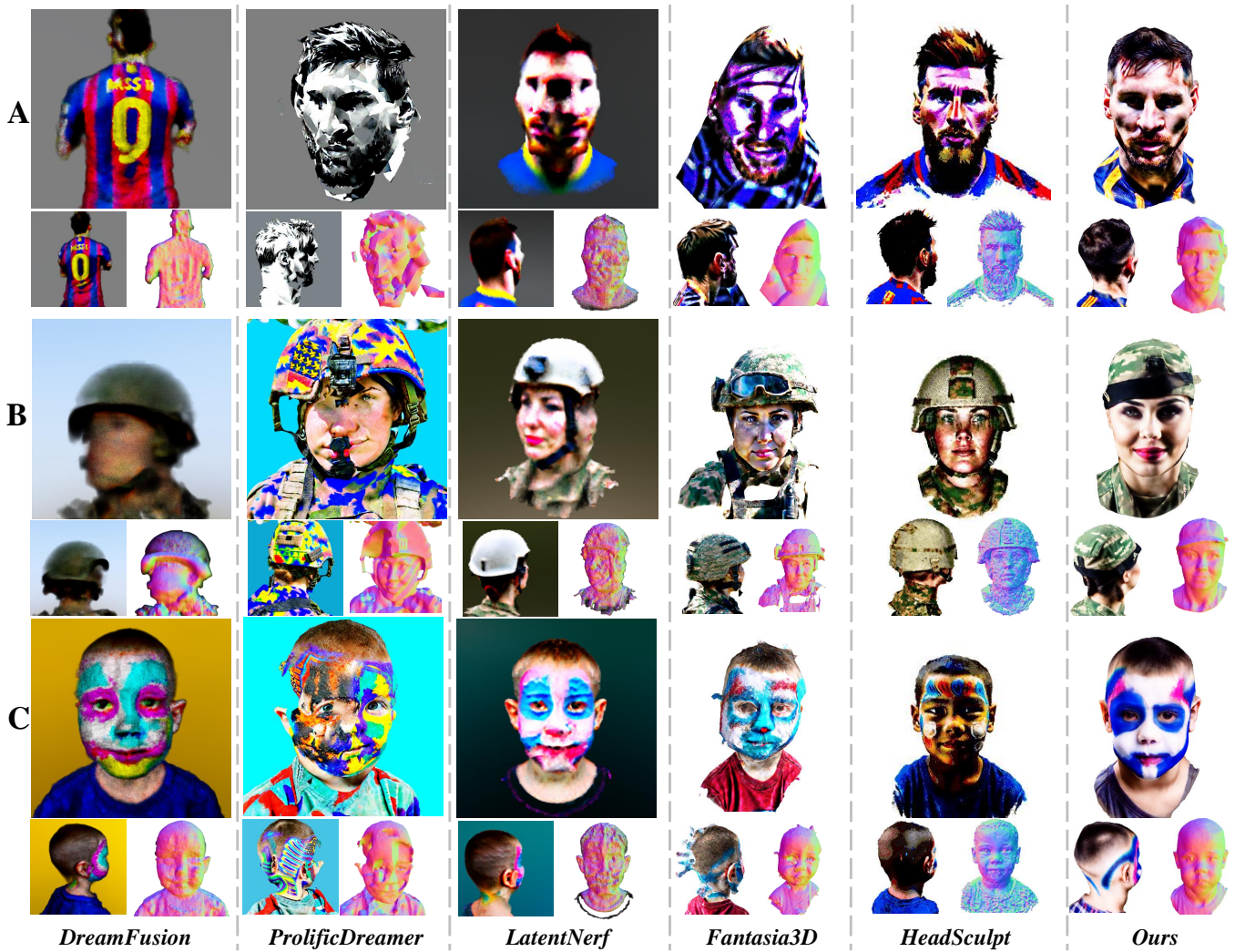


Figure 3: Qualitative comparison with SOTA methods. Text Prompts: (A) a DSLR portrait of Lionel Messi. (B) a DSLR portrait of a female soldier, wearing a helmet. (C) a DSLR portrait of a boy with facial painting. Overall, our method demonstrates superior fidelity in terms of both geometry and textures.



Figure 4: The editing results of our HeadArtist. Our approach enables the manipulation of geometry and textures, thereby aligning the resulting content with the corresponding human-language descriptions.

text-to-image diffusion model and LoRA model, respectively, which follows VSD. In (b), we replace ϵ_{π} with a 2D text-to-image diffusion model. The results in (a) and (b) show that multi-face Janus

artifacts occur (i.e., two brims with Obama) and poor performance for texture and geometry coherence. These two configurations can be regarded as distilling the 3D head with a 2D diffusion model. As

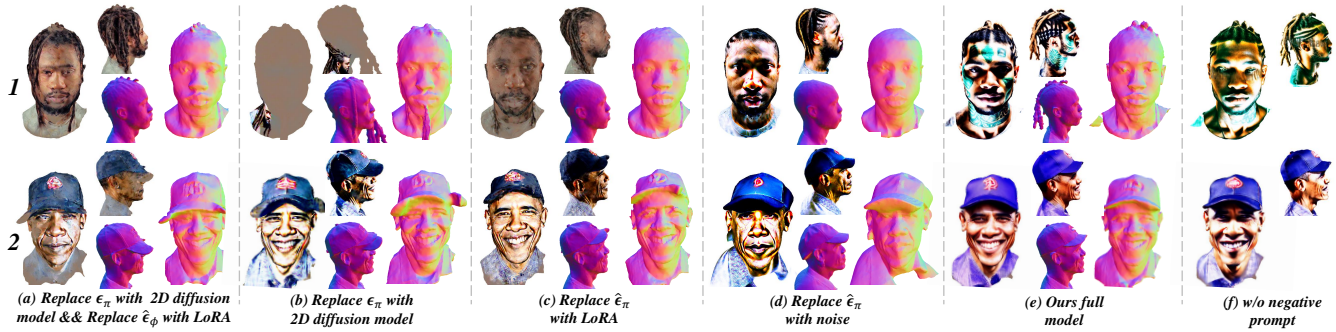


Figure 5: Ablation study. Text Prompts: 1) a DSLR portrait of a young man with dreadlocks; 2) a DSLR portrait of Obama with a baseball cap. Compared with (a), (b), and (c), our full configuration in (e) avoids the multi-face Janus problems (e.g., multiple brims of Obama). Meanwhile, (e) can generate complex geometries which are better match the text (i.e., (a)~(d) can not generate the dreadlocks). Besides, (e) predicts more natural and fidelity colors and helps the texture fit the geometry better than (d). (f) shows our results without negative prompts.

the 2D diffusion model lacks prior knowledge of heads and cannot be guided by the camera, the performance is limited. In (c), we change $\hat{\epsilon}_\pi$ to LoRA. In (d), we replace $\hat{\epsilon}_\pi$ by noise following SDS, and we set CFG of ϵ_π to 100. These two configurations yield better results than (a) and (b). This is because the target distribution of (c) and (d) is a 3D head-aware diffusion model. Nonetheless, due to the spatial mismatch of noise during gradient calculation of (c), the predicted results still exhibit the multi-face Janus issue. And (d) suffers from over-saturation and over-smoothing with large CFG, which are the inherent problems of SDS. In contrast, our full configuration (e) achieves better performance in both geometry (i.e., able to generate dreadlocks) and texture with SSD, which leverages head prior knowledge effectively and benefits from the spatial alignment of the predicted scores from two identical ControlNets. We also provide the corresponding quantitative results in Table. 2.

5.4.2 Effectiveness of Negative Prompts. We observe that our method can directly employ negative prompts to improve further performance. Without the use of negative prompts, as shown in (f) of Figure 5, our method tends to exhibit slight over-exposure and may introduce artifacts (i.e., there are some texts printed on the face of the first man). This artifact is also observed in the 2D images generated by ControlNet if negative prompts are not employed. By using negative prompts, we have improved the quality of the generated content while effectively reducing artifacts. We also provide the corresponding quantitative results in Table. 2 of supplementary.

6 LIMITATIONS

Our method currently cannot achieve the photorealism of 3D head reconstruction methods or 3D GANs. Additionally, it is difficult to generate some characters with complex structures in Japanese animation (e.g., KINOMOTO SAKURA in Fig. 6). This is because FLAME initializes our model, and no geometric priors of Japanese anime characters are introduced. Moreover, the diffusion model we used is not good at generating Japanese animation characters. Meanwhile, our method can change the expression of the character, but we cannot drive the 3D head directly, which is also one of our future works.



Figure 6: The failure results of our method. We find our method can not handle such complex Japanese animation characters well.

7 CONCLUSION

We propose HeadArtist with Self Score Distillation (SSD) to generate the high-fidelity 3D human heads with language expressions. Our SSD utilizes a landmark-guided ControlNet twice to predict the distribution scores of the optimized and target heads, respectively. Then, we minimize the distance of these two scores to update the parameters of the 3d head. The two scores are spatially aligned to avoid the multi-face Janus issue. Meanwhile, the landmark introduces facial semantics. Moreover, we can utilize the negative prompts to enhance the texture quality. Experiments on diverse text prompts demonstrate the significant performance of our method. Finally, we extend the SSD to general object generation by replacing the ControlNet with other 3D-aware diffusion models (i.e., MVDream [Liu et al. 2023b]) in supplementary. This attempt could bring a new perspective to 3D generation.

ACKNOWLEDGMENTS

This project was supported by the National Key R&D Program of China under grant number 2022ZD0161501.

REFERENCES

- Shivangi Aneja, Justus Thies, Angela Dai, and Matthias Nießner. 2023. Clipface: Text-guided editing of textured 3d morphable models. In *ACM SIGGRAPH 2023 Conference Proceedings*. 1–11.
- Volker Blanz and Thomas Vetter. 2023. A morphable model for the synthesis of 3D faces. In *Seminal Graphics Papers: Pushing the Boundaries, Volume 2*. 157–164.
- Yukang Cao, Yan-Pei Cao, Kai Han, Ying Shan, and Kwan-Yee K Wong. 2023. DreamAvatar: Text-and-shape guided 3d human avatar generation via diffusion models. *arXiv preprint arXiv:2304.00916* (2023).
- Rui Chen, Yongwei Chen, Ningxin Jiao, and Kui Jia. 2023. Fantasia3d: Disentangling geometry and appearance for high-quality text-to-3d content creation. *arXiv preprint arXiv:2303.13873* (2023).
- CrucibleAI. 2023. ControlNetMediaPipeFace. <https://huggingface.co/CrucibleAI/ControlNetMediaPipeFace>.
- Patrick Esser, Johnathan Chiu, Parmida Atighehchian, Jonathan Granskog, and Anastasia Germanidis. 2023. Structure and content-guided video synthesis with diffusion models. In *Proceedings of the IEEE/CVF International Conference on Computer Vision*. 7346–7356.
- Ian Goodfellow, Jean Pouget-Abadie, Mehdi Mirza, Bing Xu, David Warde-Farley, Sherjil Ozair, Aaron Courville, and Yoshua Bengio. 2014. Generative adversarial nets. *Advances in neural information processing systems* 27 (2014).
- Yuan-Chen Guo, Ying-Tian Liu, Ruizhi Shao, Christian Laforte, Vikram Voleti, Guan Luo, Chia-Hao Chen, Zi-Xin Zou, Chen Wang, Yan-Pei Cao, and Song-Hai Zhang. 2023. threestudio: A unified framework for 3D content generation. <https://github.com/threestudio-project/threestudio>.
- Xiao Han, Yukang Cao, Kai Han, Xiatian Zhu, Jiankang Deng, Yi-Zhe Song, Tao Xiang, and Kwan-Yee K Wong. 2023. HeadSculpt: Crafting 3D Head Avatars with Text. *arXiv preprint arXiv:2306.03038* (2023).
- Johnathan Ho, William Chan, Chitwan Saharia, Jay Whang, Ruiqi Gao, Alexey Gritsenko, Diederik P Kingma, Ben Poole, Mohammad Norouzi, David J Fleet, et al. 2022. Imagen video: High definition video generation with diffusion models. *arXiv preprint arXiv:2210.02303* (2022).
- Jonathan Ho, Ajay Jain, and Pieter Abbeel. 2020. Denoising diffusion probabilistic models. *Advances in neural information processing systems* 33 (2020), 6840–6851.
- Jonathan Ho and Tim Salimans. 2022. Classifier-free diffusion guidance. *arXiv preprint arXiv:2207.12598* (2022).
- Fangzhou Hong, Mingyuan Zhang, Liang Pan, Zhongang Cai, Lei Yang, and Ziwei Liu. 2022. Avatarclip: Zero-shot text-driven generation and animation of 3d avatars. *arXiv preprint arXiv:2205.08535* (2022).
- Edward J Hu, Yelong Shen, Phillip Wallis, Zeyuan Allen-Zhu, Yuanzhi Li, Shean Wang, Lu Wang, and Weizhu Chen. 2021. Lora: Low-rank adaptation of large language models. *arXiv preprint arXiv:2106.09685* (2021).
- Shuo Huang, Zongxin Yang, Liangting Li, Yi Yang, and Jia Jia. 2023b. AvatarFusion: Zero-shot Generation of Clothing-Decoupled 3D Avatars Using 2D Diffusion. In *Proceedings of the 31st ACM International Conference on Multimedia*. 5734–5745.
- Xin Huang, Ruizhi Shao, Qi Zhang, Hongwen Zhang, Ying Feng, Yebin Liu, and Qing Wang. 2023a. HumanNorm: Learning Normal Diffusion Model for High-quality and Realistic 3D Human Generation. *arXiv preprint arXiv:2310.01406* (2023).
- Yangyi Huang, Hongwei Yi, Yuliang Xiu, Tingting Liao, Jiayang Tang, Deng Cai, and Justus Thies. 2023c. TeCH: Text-guided Reconstruction of Lifelike Clothed Humans. *arXiv preprint arXiv:2308.08545* (2023).
- Ajay Jain, Ben Mildenhall, Jonathan T Barron, Pieter Abbeel, and Ben Poole. 2022. Zero-shot text-guided object generation with dream fields. 2022 IEEE. In *CVF Conference on Computer Vision and Pattern Recognition (CVPR)*. 857–866.
- Nikos Kolotouros, Thiemo Alldieck, Andrei Zanfir, Eduard Gabriel Bazavan, Mihai Fieraru, and Cristian Sminchisescu. 2023. DreamHuman: Animatable 3D Avatars from Text. *arXiv preprint arXiv:2306.09329* (2023).
- Samuli Laine, Janne Hellsten, Tero Karras, Yeongho Seol, Jaakko Lehtinen, and Timo Aila. 2020. Modular Primitives for High-Performance Differentiable Rendering. *ACM Transactions on Graphics* 39, 6 (2020).
- Tianye Li, Timo Bolkart, Michael J Black, Hao Li, and Javier Romero. 2017. Learning a model of facial shape and expression from 4D scans. *ACM Transactions on Graphics, (Proc. SIGGRAPH Asia)* 36, 6 (2017), 194:1–194:17. <https://doi.org/10.1145/3130800.3130813>
- Yixun Liang, Xin Yang, Jiantao Lin, Haodong Li, Xiaogang Xu, and Yingcong Chen. 2023. Lucidreamer: Towards high-fidelity text-to-3d generation via interval score matching. *arXiv preprint arXiv:2311.11284* (2023).
- Chen-Hsuan Lin, Jun Gao, Luming Tang, Towaki Takikawa, Xiaohui Zeng, Xun Huang, Karsten Kreis, Sanja Fidler, Ming-Yu Liu, and Tsung-Yi Lin. 2023. Magic3d: High-resolution text-to-3d content creation. In *Proceedings of the IEEE/CVF Conference on Computer Vision and Pattern Recognition*. 300–309.
- Ruoshi Liu, Rundi Wu, Basile Van Hoorick, Pavel Tokmakov, Sergey Zakharov, and Carl Vondrick. 2023b. Zero-1-to-3: Zero-shot one image to 3d object. In *Proceedings of the IEEE/CVF International Conference on Computer Vision*. 9298–9309.
- Yuan Liu, Cheng Lin, Zijiao Zeng, Xiaoxiao Long, Lingjie Liu, Taku Komura, and Wenping Wang. 2023a. Syncdreamer: Generating multiview-consistent images from a single-view image. *arXiv preprint arXiv:2309.03453* (2023).
- Camillo Lugaresi, Jiuqiang Tang, Hadon Nash, Chris McClanahan, Esha Uboweja, Michael Hays, Fan Zhang, Chuo-Ling Chang, Ming Guang Yong, Juhyun Lee, et al. 2019. Mediapipe: A framework for building perception pipelines. *arXiv preprint arXiv:1906.08172* (2019).
- Mohit Mendiratta, Xingang Pan, Mohamed Elgharib, Kartik Teotia, Ayush Tewari, Vladislav Golyanik, Adam Kortylewski, and Christian Theobalt. 2023. Avatarstudio: Text-driven editing of 3d dynamic human head avatars. *ACM Transactions on Graphics (TOG)* 42, 6 (2023), 1–18.
- Gal Metzer, Elad Richardson, Or Patashnik, Raja Giryes, and Daniel Cohen-Or. 2023. Latent-nerf for shape-guided generation of 3d shapes and textures. In *Proceedings of the IEEE/CVF Conference on Computer Vision and Pattern Recognition*. 12663–12673.
- Oscar Michel, Roi Bar-On, Richard Liu, Sagie Benaim, and Rana Hanocka. 2022. Text2mesh: Text-driven neural stylization for meshes. In *Proceedings of the IEEE/CVF Conference on Computer Vision and Pattern Recognition*. 13492–13502.
- Ben Mildenhall, Pratul P Srinivasan, Matthew Tanicli, Jonathan T Barron, Ravi Ramamoorthi, and Ren Ng. 2021. Nerf: Representing scenes as neural radiance fields for view synthesis. *Commun. ACM* 65, 1 (2021), 99–106.
- Thomas Müller, Alex Evans, Christoph Schied, and Alexander Keller. 2022. Instant neural graphics primitives with a multiresolution hash encoding. *ACM Transactions on Graphics (ToG)* 41, 4 (2022), 1–15.
- Alex Nichol, Prafulla Dhariwal, Aditya Ramesh, Pranav Shyam, Pamela Mishkin, Bob McGrew, Ilya Sutskever, and Mark Chen. 2021. Glide: Towards photorealistic image generation and editing with text-guided diffusion models. *arXiv preprint arXiv:2112.10741* (2021).
- Georgios Pavlakos, Vasileios Choutas, Nima Ghorbani, Timo Bolkart, Ahmed AA Osman, Dimitrios Tzionas, and Michael J Black. 2019. Expressive body capture: 3d hands, face, and body from a single image. In *Proceedings of the IEEE/CVF conference on computer vision and pattern recognition*. 10975–10985.
- Ben Poole, Ajay Jain, Jonathan T Barron, and Ben Mildenhall. 2022. Dreamfusion: Text-to-3d using 2d diffusion. *arXiv preprint arXiv:2209.14988* (2022).
- Guocheng Qian, Jinjie Mai, Abdullah Hamdi, Jian Ren, Aliaksandr Siarohin, Bing Li, Hsin-Ying Lee, Ivan Skorokhodov, Peter Wonka, Sergey Tulyakov, et al. 2023. Magic123: One image to high-quality 3d object generation using both 2d and 3d diffusion priors. *arXiv preprint arXiv:2306.17843* (2023).
- Lingteng Qiu, Guanying Chen, Xiaodong Gu, Qi Zuo, Mutian Xu, Yushuang Wu, Weihao Yuan, Zilong Dong, Liefeng Bo, and Xiaoguang Han. 2023. Richreamer: A generalizable normal-depth diffusion model for detail richness in text-to-3d. *arXiv preprint arXiv:2311.16918* (2023).
- Alec Radford, Jong Wook Kim, Chris Hallacy, Aditya Ramesh, Gabriel Goh, Sandhini Agarwal, Girish Sastry, Amanda Askell, Pamela Mishkin, Jack Clark, et al. 2021. Learning transferable visual models from natural language supervision. In *International conference on machine learning*. PMLR, 8748–8763.
- Aditya Ramesh, Prafulla Dhariwal, Alex Nichol, Casey Chu, and Mark Chen. 2022. Hierarchical text-conditional image generation with clip latents. *arXiv preprint arXiv:2204.06125* 1, 2 (2022), 3.
- Aditya Ramesh, Mikhail Pavlov, Gabriel Goh, Scott Gray, Chelsea Voss, Alec Radford, Mark Chen, and Ilya Sutskever. 2021. Zero-shot text-to-image generation. In *International Conference on Machine Learning*. PMLR, 8821–8831.
- Robin Rombach, Andreas Blattmann, Dominik Lorenz, Patrick Esser, and Björn Ommer. 2022. High-resolution image synthesis with latent diffusion models. In *Proceedings of the IEEE/CVF conference on computer vision and pattern recognition*. 10684–10695.
- Chitwan Saharia, William Chan, Saurabh Saxena, Lala Li, Jay Whang, Emily L Denton, Kamyar Ghasemipour, Raphael Gontijo Lopes, Burcu Karagol Ayan, Tim Salimans, et al. 2022. Photorealistic text-to-image diffusion models with deep language understanding. *Advances in Neural Information Processing Systems* 35 (2022), 36479–36494.
- Aditya Sanghi, Hang Chu, Joseph G Lambourne, Ye Wang, Chin-Yi Cheng, Marco Fumero, and Kamal Rahimi Malekshah. 2022. Clip-forged: Towards zero-shot text-to-shape generation. In *Proceedings of the IEEE/CVF Conference on Computer Vision and Pattern Recognition*. 18603–18613.
- Tianchang Shen, Jun Gao, Kangxue Yin, Ming-Yu Liu, and Sanja Fidler. 2021. Deep marching tetrahedra: a hybrid representation for high-resolution 3d shape synthesis. *Advances in Neural Information Processing Systems* 34 (2021), 6087–6101.
- Yichun Shi, Peng Wang, Jianglong Ye, Mai Long, Kejie Li, and Xiao Yang. 2023. Mv-dream: Multi-view diffusion for 3d generation. *arXiv preprint arXiv:2308.16512* (2023).
- Uriel Singer, Adam Polyak, Thomas Hayes, Xi Yin, Jie An, Songyang Zhang, Qiyuan Hu, Harry Yang, Oron Ashual, Oran Gafni, et al. 2022. Make-a-video: Text-to-video generation without text-video data. *arXiv preprint arXiv:2209.14792* (2022).
- stabilityai. 2023. stable-diffusion-2-1-base. <https://huggingface.co/stabilityai/stable-diffusion-2-1-base/tree/main>.
- Jingxiang Sun, Bo Zhang, Ruizhi Shao, Lizhen Wang, Wen Liu, Zhenda Xie, and Yebin Liu. 2023. Dreamcraft3d: Hierarchical 3d generation with bootstrapped diffusion prior. *arXiv preprint arXiv:2310.16818* (2023).
- Jiaxiang Tang, Jiawei Ren, Hang Zhou, Ziwei Liu, and Gang Zeng. 2023. Dreamgaussian: Generative gaussian splatting for efficient 3d content creation. *arXiv preprint arXiv:2309.16653* (2023).

- Patrick von Platen, Suraj Patil, Anton Lozhkov, Pedro Cuenca, Nathan Lambert, Kashif Rasul, Mishig Davaadorj, and Thomas Wolf. 2022. Diffusers: State-of-the-art diffusion models.
- Can Wang, Menglei Chai, Mingming He, Dongdong Chen, and Jing Liao. 2022. Clipnerf: Text-and-image driven manipulation of neural radiance fields. In *Proceedings of the IEEE/CVF Conference on Computer Vision and Pattern Recognition*. 3835–3844.
- Haochen Wang, Xiaodan Du, Jiahao Li, Raymond A Yeh, and Greg Shakhnarovich. 2023a. Score jacobian chaining: Lifting pretrained 2d diffusion models for 3d generation. In *Proceedings of the IEEE/CVF Conference on Computer Vision and Pattern Recognition*. 12619–12629.
- Peng Wang, Lingjie Liu, Yuan Liu, Christian Theobalt, Taku Komura, and Wenping Wang. 2021. Neus: Learning neural implicit surfaces by volume rendering for multi-view reconstruction. *arXiv preprint arXiv:2106.10689* (2021).
- Tengfei Wang, Bo Zhang, Ting Zhang, Shuyang Gu, Jianmin Bao, Tadas Baltrusaitis, Jingjing Shen, Dong Chen, Fang Wen, Qifeng Chen, et al. 2023c. Rodin: A generative model for sculpting 3d digital avatars using diffusion. In *Proceedings of the IEEE/CVF Conference on Computer Vision and Pattern Recognition*. 4563–4573.
- Zhengyi Wang, Cheng Lu, Yikai Wang, Fan Bao, Chongxuan Li, Hang Su, and Jun Zhu. 2023b. ProlificDreamer: High-Fidelity and Diverse Text-to-3D Generation with Variational Score Distillation. *arXiv preprint arXiv:2305.16213* (2023).
- Jay Zhangjie Wu, Yixiao Ge, Xintao Wang, Stan Weixian Lei, Yuchao Gu, Yufei Shi, Wynne Hsu, Ying Shan, Xiaohu Qie, and Mike Zheng Shou. 2023a. Tune-a-video: One-shot tuning of image diffusion models for text-to-video generation. In *Proceedings of the IEEE/CVF International Conference on Computer Vision*. 7623–7633.
- Menghua Wu, Hao Zhu, Linjia Huang, Yiyu Zhuang, Yuanxun Lu, and Xun Cao. 2023b. High-fidelity 3D face generation from natural language descriptions. In *Proceedings of the IEEE/CVF Conference on Computer Vision and Pattern Recognition*. 4521–4530.
- Cuican Yu, Guansong Lu, Yihan Zeng, Jian Sun, Xiaodan Liang, Huibin Li, Zongben Xu, Songcen Xu, Wei Zhang, and Hang Xu. 2023. Towards High-Fidelity Text-Guided 3D Face Generation and Manipulation Using only Images. In *Proceedings of the IEEE/CVF International Conference on Computer Vision*. 15326–15337.
- Jiahui Yu, Yuanzhong Xu, Jing Yu Koh, Thang Luong, Gunjan Baid, Zirui Wang, Vijay Vasudevan, Alexander Ku, Yinfei Yang, Burcu Karagol Ayan, et al. 2022. Scaling autoregressive models for content-rich text-to-image generation. *arXiv preprint arXiv:2206.10789* 2, 3 (2022), 5.
- Ziyang Yuan, Yiming Zhu, Yu Li, Hongyu Liu, and Chun Yuan. 2023. Make Encoder Great Again in 3D GAN Inversion through Geometry and Occlusion-Aware Encoding. *arXiv preprint arXiv:2303.12326* (2023).
- Yifei Zeng, Yuanxun Lu, Xinya Ji, Yao Yao, Hao Zhu, and Xun Cao. 2023. AvatarBooth: High-Quality and Customizable 3D Human Avatar Generation. *arXiv preprint arXiv:2306.09864* (2023).
- Chi Zhang, Yiwen Chen, Yijun Fu, Zhenglin Zhou, Gang Yu, Billz Wang, Bin Fu, Tao Chen, Guosheng Lin, and Chunhua Shen. 2023a. StyleAvatar3D: Leveraging Image-Text Diffusion Models for High-Fidelity 3D Avatar Generation. *arXiv preprint arXiv:2305.19012* (2023).
- Huichao Zhang, Bowen Chen, Hao Yang, Liao Qu, Xu Wang, Li Chen, Chao Long, Feida Zhu, Kang Du, and Min Zheng. 2023b. Avatarverse: High-quality & stable 3d avatar creation from text and pose. *arXiv preprint arXiv:2308.03610* (2023).
- Hao Zhang, Yao Feng, Peter Kulits, Yandong Wen, Justus Thies, and Michael J Black. 2023c. Text-Guided Generation and Editing of Compositional 3D Avatars. *arXiv preprint arXiv:2309.07125* (2023).
- Longwen Zhang, Qiwei Qiu, Hongyang Lin, Qixuan Zhang, Cheng Shi, Wei Yang, Ye Shi, Sibe Yang, Lan Xu, and Jingyi Yu. 2023d. DreamFace: Progressive Generation of Animatable 3D Faces under Text Guidance. *arXiv preprint arXiv:2304.03117* (2023).
- Lvmin Zhang, Anyi Rao, and Maneesh Agrawala. 2023e. Adding conditional control to text-to-image diffusion models. In *Proceedings of the IEEE/CVF International Conference on Computer Vision*. 3836–3847.
- Yinglin Zheng, Hao Yang, Ting Zhang, Jianmin Bao, Dongdong Chen, Yangyu Huang, Lu Yuan, Dong Chen, Ming Zeng, and Fang Wen. 2022. General facial representation learning in a visual-linguistic manner. In *Proceedings of the IEEE/CVF Conference on Computer Vision and Pattern Recognition*. 18697–18709.
- Joseph Zhu and Peiye Zhuang. 2023. HiFA: High-fidelity Text-to-3D with Advanced Diffusion Guidance. *arXiv preprint arXiv:2305.18766* (2023).
- Yiming Zhu, Hongyu Liu, Yibing Song, Ziyang Yuan, Xintong Han, Chun Yuan, Qifeng Chen, and Jue Wang. 2022. One model to edit them all: Free-form text-driven image manipulation with semantic modulations. *Advances in Neural Information Processing Systems* 35 (2022), 25146–25159.



‡ an middle aged Asian woman with short hair, angry expression



‡ a young man with curly hair wearing glasses



‡ Julius Robert Oppenheimer



† Stormtrooper



‡ Iron Man



† Arthas Menethil



† Elsa in Frozen



† Illidan Stormrage



‡ an elderly woman with deep wrinkles, wearing a knitted hat



‡ an overweight Asian man with a crown-braid hairstyle



‡ Gandalf wearing wizard hat



‡ an old bald man with short beard



‡ a young woman with Mohawk Haircuts



‡ Captain America



‡ Daenerys Targaryen



† RX-0 Unicorn Gundam

Figure 7: More generation results of HeadArtist. Our method preserves remarkable performance on both authentic human and cartoon character heads generation. † and ‡ denote the prefixes “a head of ...” and “a DSLR portrait of ...”, respectively.

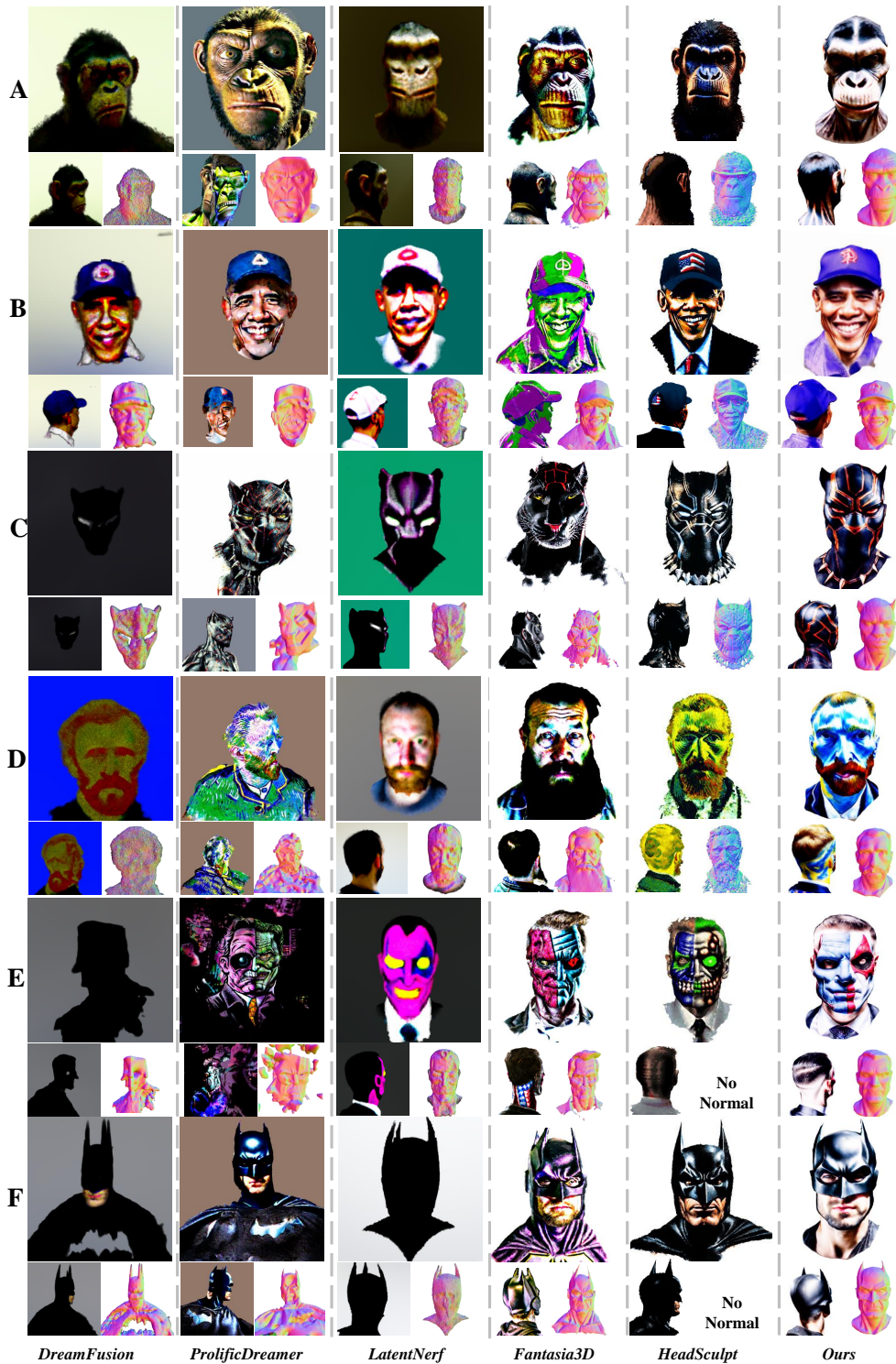


Figure 8: More qualitative comparison. Text Prompts: (A) a DSLR portrait of Caesar in Rise of the Planet of the Apes. (B) a DSLR portrait of Obama with a baseball cap. (C) a DSLR portrait of Black Panther in Marvel. (D) a portrait of Vincent Van Gogh. (E) a DSLR portrait of Two-Face in DC. (F) a DSLR portrait of Batman. Visually, our method generates more reasonable geometry and high-quality texture, and the generated 3D heads are more consistent with the corresponding text prompts.

In this supplementary, we first show that our method can effectively address the Janus problem in general object generation. Then, we provide visual comparison results between RichDreamer, LucidDreamer, HumanNorm, Magic123, and Our method. The results demonstrate the excellent performance of our method. Furthermore, we discuss the limitations of our method and display the result when our method abandons the texture step or utilizes other 3D representations. Meanwhile, we provide more details of our method, including pseudocode, 3D representation initialization, and the weights for each loss item. Finally, we show diverse results when we use the same prompt as guidance.

A RESOLVING THE JANUS PROBLEM IN GENERAL OBJECT GENERATION WITH SSD

We replace the Controlnet with MVDream and the DMTed with Nerf for general object generation. Meanwhile, the geometry and texture are generated together in a single step, similar to the DreamFusion. And we initialize the Nerf with spatial density bias following the Magic3D. For fair comparisons, we use the results on the project page of MVDream for all comparable methods (i.e., DreamFusion, Magic3D, Text2Mesh, ProlificDreamer, and MVDream). The results are shown in Fig. 11. Apart from the MVDream and MVDream+SSD, the other methods all have the Janus problem. This is because the MVDream is a multi-view diffusion model, which brings the pose information during the generation process to alleviate the Janus problem. However, MVDream utilizes the SDS directly for 3D asset generation in the original paper, which causes the results to be unreal and over-saturation (e.g., the unnatural texture in b of MVDream). In contrast, we can produce more reasonable textures and address the Janus problem at the same time, which proves the advantages of our approach (e.g., more real results in b of MVDream+SSD).

B VISUAL COMPARISON WITH MORE METHODS

We compare our method with RichDreamer, LucidDreamer, HumanNorm, and Magic123 in Fig. [?]. The HumanNorm can produce good results, but the content is not real (i.e., not fidelity texture in b of HumanNorm) and the geometry seems distorted (i.e., exaggerated geometry in c of HumanNorm). The LucidDreamer generates the results with both strange colors and over-saturation. For Magic123, we generate the input image with ControlNet and the corresponding text prompt. We find the results of Magic123 suffers from the Janus problem and over-smooth. RichDreamer performs well in c, but the geometry has artifacts (i.e., the head of c in RichDreamer is not completed). For the a and b, RichDreamer shows bad performance (i.e., the artifacts in both eyes in a and the unreal content in b). In contrast to these baselines, our method generates human heads with more fidelity texture and reasonable geometry simultaneously.

C NECESSITY OF TEXTURE STEP AND UTILIZING OTHER 3D REPRESENTATION

We merge the texture and geometry generation in one step, as shown in Fig. 9. We find our method can produce good texture but the geometry is hard to optimize (e.g., the geometry is similar to

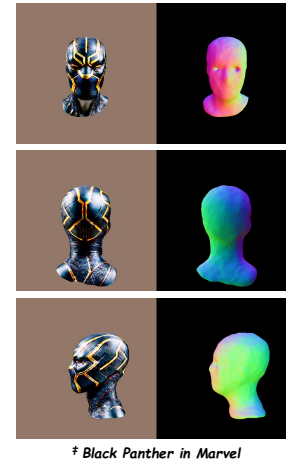


Figure 9: The generation results when HeadArtist merges the texture and geometry steps. We find the geometry is hard to optimize. During the generation, we set the CFG to 7.5 to avoid over-saturation and over-smooth, but geometry needs a large CFG for stable training since there is a domain gap between the real image and the normal map.

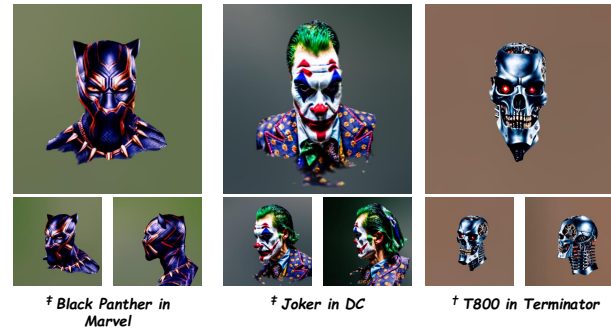


Figure 10: The generation results when HeadArtist utilizes NeRF representation. The good performance shows our method can be adapted to different representations.

the shape of Flame). To merge the two steps more efficiently, we replace the DMTed with NeRF for our head generation. The results are shown in Fig. 10, and our HeadArtist can provide plausible geometry and fine detail texture.

D MORE DETAILS

We describe the pseudocode in Algorithm 1. The `min_step` and `max_step` are the maximize and minimize noise levels, respectively. For the first 5000 iterations, the `max_step` is 980, then it will decrease to 700 to make the training focus on detail generation similar to the ProlificDreamer. During the geometry generation, we use two common regularization losses, including normal consistency and Laplacian smoothness. The weights of these two losses are 8000 and 10000, respectively. For the geometry initialization, we randomly select 10000 points for each iteration, and we minimize the distance

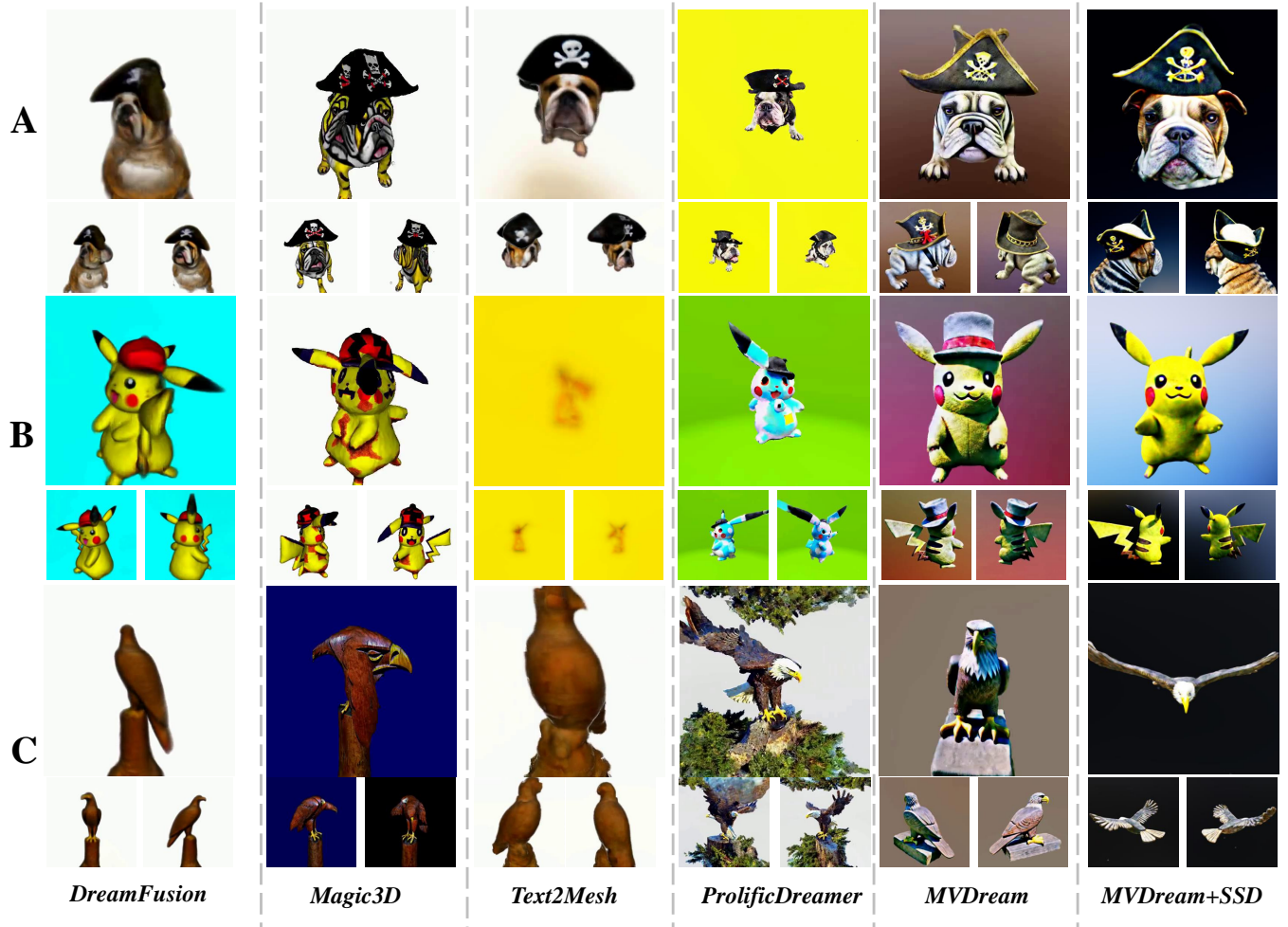


Figure 11: Text Prompts: (A) A bulldog wearing a black pirate hat. (B) A bald eagle carved out of wood. (C) Pikachu with hat. Overall, MVDream+SSD demonstrates superior fidelity in terms of both geometry and textures.

ALGORITHM 1: Self Score Distillation.

```

def self_score_distillation(landmark  $c_L$ , ControlNet,
rendered_image, text  $y$ , negative_text  $y_{neg}$ ):
    t = torch.randint(min_step, max_step)
    noise = torch.randn_like(rendered_image)
     $x_t$  = rendered_image + noise
    noise_pretrain = Controlnet( $x_t$ ;  $y$ ,  $y_{neg}$ ,  $t$ ,  $c_L$ ,  $CFG = 7.5$  or  $100$ )
    noise_head = Controlnet( $x_t$ ;  $y$ ,  $t$ ,  $c_L$ ,  $CFG = 1$ )
    grad = noise_pretrain - noise_head
    target = (rendered_image - grad).detach()
    loss = MSE(rendered_image, target)

```

between the sdf value of these points from the Flame model and optimize DMTed. For the texture, we set the maximum time steps as 0.98, and we decrease it to 0.7 after 5000 iterations for detail

generation similar to ProlificDreamer [Wang et al. 2023b]. For the camera sampling, we set the camera distance range as 3, set the FOV range as (30, 50), and set the elevation range as (-10, 45).

Finally, we follow HIFA [Zhu and Zhuang 2023] to calculate the SSD in image space with around 900 iterations after the texture generation to get better performance.

E DIVERSE RESULTS

In Fig. 13, we show our method can generate diverse results with the same prompts, which demonstrates the robustness of our method.

F MORE EDITING RESULTS

Figure 14 demonstrates our ability to edit 3D head models in terms of geometry and texture effectively.

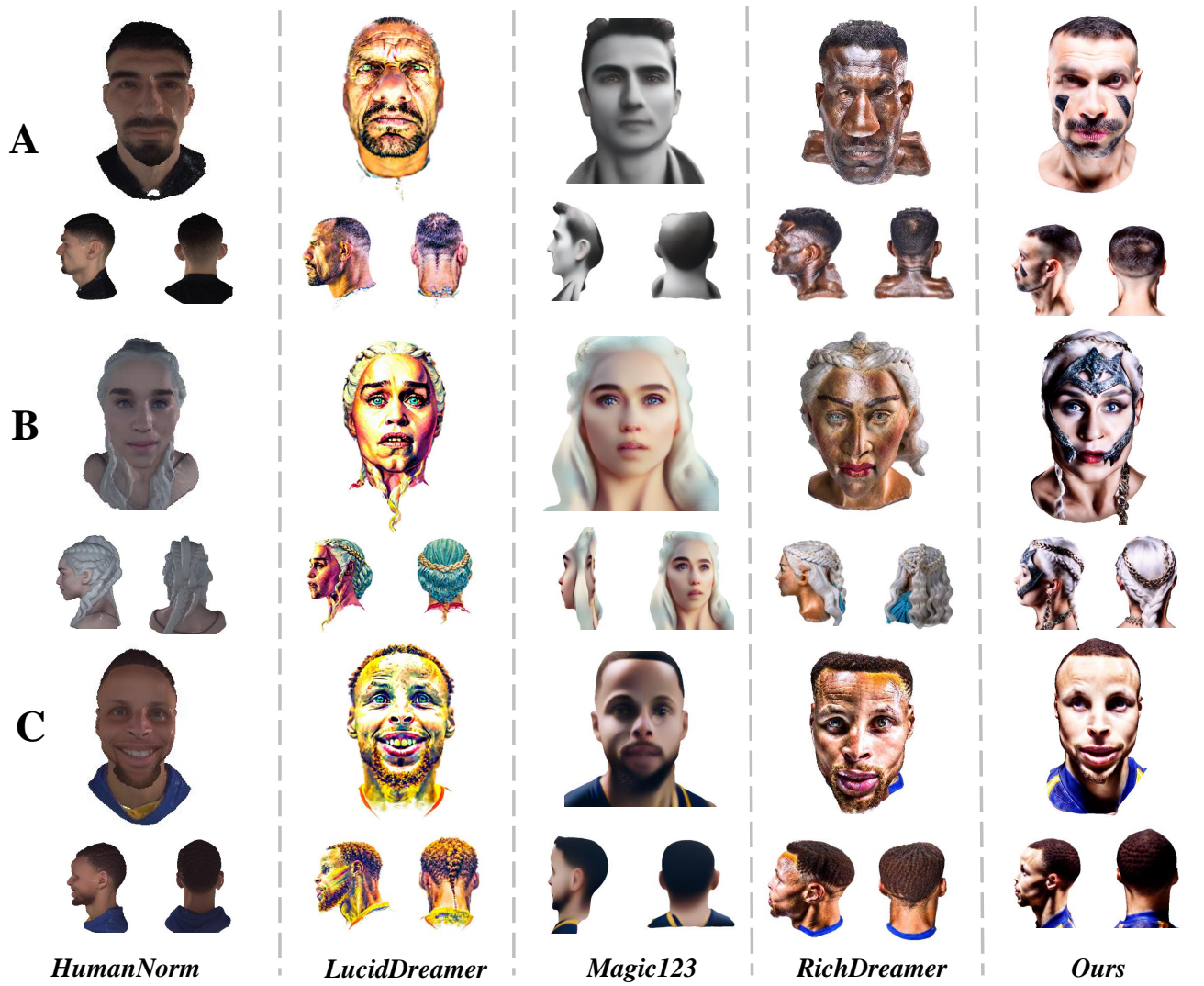


Figure 12: Text Prompts: (A) a DSLR portrait of a man with a square jaw. (B) a DSLR photo of Leonardo DiCaprio (C) a DSLR photo of Stephen Curry. Overall, our method demonstrates superior fidelity in terms of both geometry and textures.



Figure 13: The diverse results of our method. Our method can produce different high quality results with a single text prompt. † and ‡ denote the prefixes “a head of ...” and “a DSLR portrait of ...”, respectively.



Figure 14: More editing results of HeadArtist. Our method can effectively modify the texture and geometry to match the corresponding text semantics. Text in orange denotes the editing instruction.